Cross-Eyed 2017: Cross-Spectral Iris/Periocular Recognition Competition

Ana F. Sequeira[1], Lulu Chen[1], James Ferryman[1], Peter Wild[2],
Fernando Alonso-Fernandez[3], Josef Bigun[3], Kiran B. Raja[4], R. Raghavendra[4], Christoph Busch[4],
Tiago de Freitas Pereira[5], Sébastien Marcel[5], Sushree Sangeeta Behera[6], Mahesh Gour[6], Vivek Kanhangad[6],
[1] University of Reading, UK, {a.f.p.sequeira,l.chen,j.m.ferryman}@reading.ac.uk
[2]Tecan Austria GmbH, Austria, Peter.Wild@tecan.com
[3]Halmstad University, Sweden {feralo,josef.bigun}@hh.se
[4]Norwegian Biometrics Laboratory, NTNU, Norway,
{kiran.raja,raghavendra.ramachandra,christoph.busch}@ntnu.no
[5]Idiap Research Institute, Switzerland {tiago.pereira,sebastien.marcel}@idiap.ch
[6]Indian Institute of Technology Indore, India {mt1502102010,maheshg,kvivek}@iiti.ac.in

Abstract

This work presents the 2^{nd} Cross-Spectrum Iris/Periocular Recognition Competition (Cross-Eyed2017). The main goal of the competition is to promote and evaluate advances in cross-spectrum iris and periocular recognition. This second edition registered an increase in the participation numbers ranging from academia to industry: five teams submitted twelve methods for the periocular task and five for the iris task. The benchmark dataset is an enlarged version of the dual-spectrum database containing both iris and periocular images synchronously captured from a distance and within a realistic indoor environment. The evaluation was performed on an undisclosed test-set. Methodology, tested algorithms, and obtained results are reported in this paper identifying the remaining challenges in path forward.

1. Introduction

The human iris is considered as one of the most accurate biometric characteristics but the accuracy obtained is highly impacted when the acquisition is done in less constrained environments. When it is too challenging to obtain sufficient quality for reliable iris recognition, the periocular area becomes an interesting alternative [6, 24]. The periocular biometric trait includes the surrounding features of the eye region and facilitates an improved performance for low quality iris, face or partial face images acquired with less constrained conditions, such as from a distance or on the move [24]. Most of the commercial deployments of iris recognition use images acquired in the Near Infra-Red (NIR) spectrum as this is regarded to capture the iris pattern details even for heavily pigmented iris. Nevertheless, in some situations the use of noisy images captured in the visible (VIS) spectrum has a considerable interest. It is a fact that pigmentation and specular reflections impact negatively the quality of highly pigmented irises when captured under VIS light. VIS imaging can highlight the iris texture with similar quality as compared to under NIR illumination for light pigmented irises. The choice of a particular illumination is then based on a trade-off between the image quality required for the specific recognition system and the practical aspects of the real-world application. In some situations, like surveillance and border control, it may happen that the NIR images captured in the enrolment phase with controlled conditions should be compared against images captured under VIS illumination in a less constrained environment. The cross-spectral comparison is gaining interest for ocular traits and others like face [8, 9, 10].

The Cross-Eyed competitions target the iris and periocular recognition tasks with the additional feature of performing cross-spectral comparison. Cross-spectral recognition has gained interest and the state-of-the-art results have underlined how this is a challenging topic in ocular recognition. Compared to the first edition, this second competition received a more representative participation from industry to academia with an increase from 2 teams participating in the *Cross-Eyed2016* edition to 5 teams in this *Cross-Eyed2017* edition. The 5 teams contributed to the periocular task with a total of 12 methods and 2 teams contributed with 5 methods to the iris task.

This paper presents the second edition of the Cross-Eyed competition[1] by summarising he methods are summarised and the results presented. The key contributions of this

[1]Information available at www.crosseyed.eu.

work are:

- An enlarged database for cross-spectral iris/periocular recognition distributed to the participants to support the research on the topic.
- Trustworthy benchmark results are obtained through a public competition by evaluating the methods submitted by participants on an unknown dataset.

The remainder of the paper presents: an overview of cross-spectral ocular recognition in Section 2; the details of the competition in Section 4 and, in Section 3, the benchmark dataset. A brief description of the methods submitted to the competition is given in Section 5 and the results obtained are discussed in Section 6. Finally, in Section 7 the conclusions and future challenges are envisaged.

2. Cross-Spectral Recognition

Various works have explored multi-spectral and cross-spectral techniques from different perspectives. Works can be found that propose to enhance accuracy by combining data from multispectral iris images [21]; or when information from NIR+VIS bands is combined [7]; or by the fusion of multiple spectra wavelengths [29]. Besides the fusion of information from different spectra, later works studied iris cross-spectral comparison [27, 33]. According to [27], even though the comparisons in near infrared and visible channels are independently quite accurate, the performance of cross-spectral iris matching is significantly degraded in the NIR to VIS comparison and an Equal Error Rate (EER) value of 34% is reported. More recent works show improved accuracies nevertheless corroborating the idea that this is a challenging task. An EER of 6.81% for the cross-spectral comparison NIR versus VIS is presented in [2] improving the value of 27.46% [1] (both values corresponding to the comparison NIR versus Red channel). A higher value of 33.89% for EER along with a value of 58.8% for the Genuine Acceptance Rate (GAR) at False Acceptance Rate (FRR) equal to 0.01% are reported in [20].

When compared to face and iris, the periocular cross-spectrum comparison is an even less studied task. The first study showed how challenging it is by reporting values below 50% for the verification accuracy at 1% FAR in the NIR to VIS comparison [32]. More recently, the use of Markov Random Fields and three patch Local Binary Patterns is proposed [28]. In a more recent work, an EER of 1.26% and a value of 96.04% for Genuine Match Rate (GMR) at 0.01% False Match Rate (FMR) are obtained by using Binarized Statistical Image Features along with the χ^2 distance metric and simple fusion [26]. An even more challenging problem involves matching the ocular region of a face image obtained in the VIS spectrum with an iris image obtained in the NIR spectrum [15].

For the development of new techniques, in any topic of the biometric field, the existence of suitable databases is paramount. Multi-spectral iris data is presented in [7] where each iris snapshot outputs data acquired by four different spectral channels: NIR, R, G and B, perfectly registered and synchronized. The UTIRIS database [12] comprises NIR and VIS images of the same iris however captured at different times with two devices. The PolyU Cross-Spectral Iris Database [27] comprises NIR and VIS images acquired simultaneously. The first periocular cross-spectrum database [32] comprises images from three individual spectra: VIS, night vision, and NIR. The Cross-Eyed DB [30] presented some novel features by providing images synchronously acquired in both NIR $\&$ VIS spectra and comprising respective iris and ocular regions.

3. Benchmark dataset: Cross-Eyed DB

The Reading Cross-Spectral Iris/Periocular Dataset (Cross-Eyed DB) [30, 31] is composed by both VIS and NIR images captured with a custom developed dual spectrum imaging sensor, depicted in Figure 1(a), which acquires NIR and VIS images synchronously by high-resolution (2K x 2K) machine vision cameras. The main key features of this database are:

- Cross-spectrum - synchronised NIR + VIS images;
- Images acquired from distance: 1.5 metres;
- Uncontrolled realistic indoor environment;
- Realistic and challenging illumination reflection;
- Variation in ethnicity and eye colour;
- Age range from 18 to 70 years;
- Male/female distribution $65\%/35\%$.

The Cross-Eyed DB is composed by 3 subsets: ocular, periocular (ocular with masked iris and sclera) and iris images obtained by manually cropping the face images. The 175 individuals provided 8 NIR and 8 VIS images of each eye pattern therefore each dataset is composed by 5600 eye impressions (given by $175(individuals) \times 2(eyepatterns) \times 2(spectra) \times 8(images)$). The ocular (and periocular) images are 900×800 pixels and the iris images are 400×300 pixels. In Figure 1(b), the dual spectrum versions of the same eye pattern are shown in its ocular, periocular and iris variations.

The periocular images are obtained from the ocular images by positioning a mask on the whole iris and sclera region (in line with the previous work [23]). The masking on the iris region is used firstly to ensure that periocular recognition is not achieved by using captured high quality iris pattern. This also allows a performance comparison between iris recognition and recognition using the surrounding eye region (periocular) excluding the iris (or even the

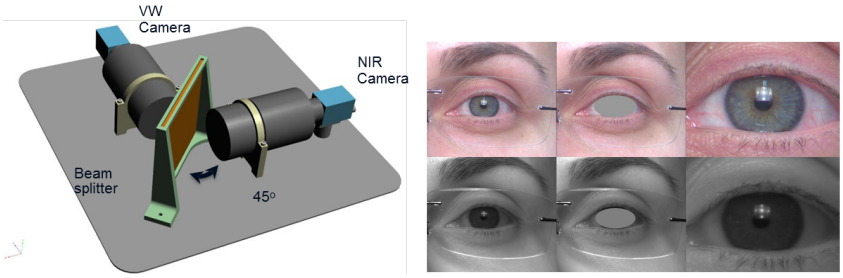

(a) (b)

Figure 1. a) Dual Sensor b) Ocular, Periocular and Iris (VIS & NIR) Cross-Eyed DB images examples.

sclera) pattern. Even though it is not likely to find perfect replicas of the occlusion resulting of the employed masking in any real-world scenario, the fact is that in real-world applications it is very common to capture the iris and the sclera with such low quality that recognition is not possible based on those regions, whether it is caused by low resolution, motion blur, high pigmentation of iris or reflections. The division in training and test sets was made as follows.

- Training set: comprises the images from 120 individuals and was released to the participants to allow the training of the methods.[2]
- Test set: comprises the images from 55 subjects and was not released and was used by the organizers to evaluate the methods submitted by the participants.

4. *Cross-Eyed2017* competition

4.1. Participants

The *Cross-Eyed2017* competition received 18 registrations from researchers all over the globe. Among the registered participants, 6 teams submitted their algorithms.[3] In this paper are presented the results of the methods submitted by: **IDIAP** from Switzerland; **IIT Indore** from India; **HH** from Halmstad University, Sweden; **NTNU** from Norwegian Biometrics Laboratory, Norwegian University of Science and Technology, Norway; and **Anonymous**.

4.2. Evaluation methodology

The *Cross-Eyed2017* competition included two intermediate submissions and one final submission. The participants were asked to submit their methods and the organizers were responsible for running the methods on the selected datasets and obtain the results. The intermediate evaluations were meant to stimulate interaction with the event, to give feedback to the participants about their performance and to allow refinement of the algorithms. The intermediate evaluations were made on the same set of 20 randomly chosen subjects. The final evaluation was made on a test dataset with 55 subjects resulting in 110 unique ocular instances.

The evaluation of the methods was carried out on two disjoint sets of enrolment and probe data. Firstly, templates were obtained for all images in both enrolment and probe sets. Then 2 types of comparisons were made: *intra-class* and *inter-class* comparisons. To perform the comparisons between the periocular images, the left eye images are compared only with left eye images and the same for the right side eye images. For the *intra-class* (same subject comparisons), every NIR image is compared against each VIS image of the same eye pattern. For the *inter-class* (different subjects comparisons), 3 random NIR images of one eye pattern are compared against 3 random VIS images of all the other eye patterns (of the same side). In the inter-class comparisons only 3 images are compared (instead of the 8 available) due to the computational effort of comparing all images.

4.3. Evaluation metrics

To comply with the ISO/IEC standards [13], the *Generalized False Accept Rate (GFAR)* and *Generalized False Reject Rate (GFRR)* evaluation metrics were used. They generalize the False Match Rate (FMR) and the False Non-Match Rate (FNMR) to include the *Failure To Acquire (FTA)* and *Failure To Enrol (FTE)* rates, and are defined as:

$$GFAR = \alpha \times \beta \times FMR \quad (1)$$

$$GFRR = FTE + \beta \times FTA + \alpha \times \beta \times FNMR \quad (2)$$

where $\alpha = 1 - FTA$ and $\beta = 1 - FTE$.

To compare the algorithms, the $GFRR@GFAR = 0.01$ is used, indicated as GF2. The EER is reported to indicate the symmetrical accept and reject rates. Also the computational time for enrolment and comparison is listed for each algorithm. The processing time for all the submitted algorithms was measured using the same machine (Intel Xeon CPU E5-2687W v2 @ 3.40GHz dual processors). Most

[2]This dataset is available upon request at www.crosseyed.eu.

[3]One team did not submit a method compliant to the guidelines so was not included in the final results nor in this paper and another team did not wish to have their identity and method description included in this paper.

teams submitted their enrol and matching programs as Windows executables, except IDIAP team that submitted their algorithms with a open source Python package which can be only run under Linux environment. It is interesting to compare the processing time among these teams despite different formats and programming languages used by the teams.

5. Methods submitted

5.1. HH methods

The HH system exploits the fusion of algorithms based on Symmetry Patterns (SAFE) [19], Gabor Spectral Decomposition (GABOR) [3], SIFT [5], Local Binary Patterns (LBP), and Histogram of Oriented Gradients (HOG) [23]. The scores of individual systems are then mapped to a log-likelihood ratio according to the probabilistic Bayesian framework [4]. Instead of mapping scores of each system separately, and then summing all scores together (as in the earlier contribution [30]), a unique mapping function is now trained with scores from all the systems to be fused. This solution is less flexible, since the mapping function is different depending on the systems to be fused, but our experiments show that it results in better recognition results. The fusion functions are trained with scores obtained by comparing images both from the same sensor and from different sensors, to cope with same and cross spectrum comparisons. Another improvement is that the fusion functions have been trained using a bigger dataset. The HH algorithms are based on different feature fusions: HH_1 (all features), HH_2 (SAFE+GABOR+LBP+HOG) and HH_3 (GABOR+LBP+HOG).

5.2. IDIAP methods

The $IDIAP$ team provided 3 periocular recognition systems[4]: based on Intersession Variability Modelling ($IDIAP_1$) and based on Geodesic Flow Kernel with Gabor jets ($IDIAP_2$ and $IDIAP_3$). Built on top of Gaussian Mixture Models (GMM), Intersession Variability Modelling (ISV) proposes to explicitly model the variations between different modalities by learning a linear subspace in the GMM supervector space. These variations are compensated during the enrolment and testing time. For this input, the periocular images are resized to 90×90 pixels and sampled in patches of 12×12 pixels moving the sampled window in one pixel. Then each patch is mean and variance normalized and the first 45 DCT coefficients are extracted. The Universe Background Model (UBM) is modelled with 512 Gaussians and the dimension of the session variability matrix (U) is 160. Implementation details of this input can be found in [25]. The Geodesic Flow Kernel (GFK) models the source domain and the target domain with d-dimensional linear subspaces and embeds them onto a Grassmann manifold. Then a Geodesic Flow [11] between these two subspaces (G) is built and an infinite number of subspaces is integrated along the flow. A grid of Gabor jets along the periocular image are used as features. A comparison between two grids of Gabor jets from visible light and near infra-red respectively S_n and T_n can be done as simple kernalized dot product between each jet (n) in the grid as following: $\frac{\sum_{n=1}^{N} S_n \cdot G \cdot T_n}{N}$.
$IDIAP$ also submitted open-source software along with the submission. Even though this was not a requirement, it is highly appreciated by all the research community. Further, the future editions of this competition will request the software from all participants as it contributes to reproducible research.

[4]The source code for these implementations can be obtained in https://pypi.python.org/pypi/bob.bio.pericrosseye_competition.

5.3. IIT Indore methods

The two approaches proposed by the $IIT\ Indore$ team for cross-spectral periocular matching are based on the fusion of a set of matching scores. The features employed belong to three categories namely, Local Phase Quantization (LPQ) [22] features, Gabor features [14] and Weibull distribution parameters of the sub-bands obtained through curvelet-based decomposition [34]. The LPQ and Gabor features corresponding to the query and enrolled images are matched using the cosine similarity measure, while the correlation score is computed for the Weibull features. While the first method ($IITIndore_1$) utilizes all the 3 types of features, the second method ($IITIndore_2$) utilizes only LPQ and Gabor features.

5.4. NTNU periocular methods

$NTNU$'s approach is built upon keypoint based descriptors: SIFT, SURF and KAZE denoted by $NTNU_1$, $NTNU_2$ and $NTNU_3$ respectively. Unlike the traditional approaches of using these descriptors, where the keypoints are automatically detected, NTNU employs a standard set of keypoints on the periocular image. The descriptors obtained from those keypoints are matched using a new matching algorithm which is based on region-bounded matching. For every descriptor computed, the matching is carried out with the descriptors in the neighbourhood of 10 pixels along two dimensions of the image. Further, all the images are scaled to an uniform size of 480×480 pixels and pre-processed using the block-based CLAHE for improving the details in the image before extracting the features.

5.5. NTNU iris methods

$NTNU$'s approaches for the iris task are based on the texture features obtained from Binarized Statistical Image Features (BSIF). The BSIF filters, learnt using natural images, have proven their reliability in vast image classifica-

tion problems [16, 17]. To extract the iris region, a coarse iris localisation technique based on [18] is employed. The responses from the multiple BSIF filters are concatenated as histograms that are further compared using the χ^2 distance metric. Two algorithms, represented as $NTNU_2$ and $NTNU_4$, are based on BSIF features; the algorithm represented as $NTNU_1$ uses a grid based SIFT descriptor and the $NTNU2$ is based on the SURF features, both as described in the Section 5.4.

Table 1. Performance of periocular methods (GF2, EER, enrolment time T_E and comparison time T_C).

Rank	Periocular Method	GF2 [%]	EER [%]	T_E [sec.]	T_C [sec.]
1	HH_1	0.74	0.82	17.95	0.45
2	$NTNU_1$	1.86	1.59	0.84	1.23
3	$IDIAP_2$	2.03	1.65	7.18	2.91
4	$IDIAP_3$	2.03	1.55	6.95	2.14
5	$NTNU_2$	4.19	2.75	0.81	1.19
6	$NTNU_3$	5.94	3.21	1.09	1.00
7	$IITIndore_1$	6.09	4.53	9.89	6.19
8	$IDIAP_1$	6.24	3.46	2.80	2.49
9	$IITIndore_2$	6.48	5.20	8.41	6.54
10	HH_2	14.87	9.16	17.18	0.06
11	HH_3	16.28	10.65	15.63	0.04
12	$Anonymous$	45.448	12.25	10.73	0.02

Table 2. Performance of iris methods (GF2, EER, enrolment time T_E and comparison time T_C).

Rank	Iris Method	GF2 [%]	EER [%]	T_E [sec.]	T_C [sec.]
1	$NTNU_4$	0.00	0.05	57.98	0.06
2	$NTNU_3$	8.43	5.58	1.01	1.08
3	$NTNU_1$	8.81	6.19	0.87	1.31
4	$Anonymous$	10.63	7.84	1.69	0.07
5	$NTNU_2$	12.77	7.95	59.09	0.05

6. Results and discussion

The evaluation of the methods is comprised of enrolment and probe template comparison and was carried out on two disjoint sets of enrolment and probe data. The first step was to obtain the templates for all images in both enrolment and probe sets. Then 2 types of comparisons were made: *intra-class* and *inter-class*. For the intra-class (or same subject comparisons), every NIR image is compared against each VIS image of the same eye pattern. For the *inter-class* (or different subjects comparisons), 3 random NIR images of one eye pattern are compared against 3 random VIS images of all the other eye patterns. In the inter-class comparisons only 3 random images (instead of the 8 available) are compared due to the computational effort of comparing all images. For the sake of equity on the comparison, all the submitted methods were evaluated using the same set of images.

Tables 1 and 2 report the ranked performance of the periocular and iris algorithms, respectively. Observing Table 1, it can be noted that the best result for the **periocular task** was achieved by the HH_1 method with a GF2 value of 0.74%. When compared to the other HH methods, it's performance is significantly better. These 3 HH methods are in all very similar and it can be inferred that this difference is due to the use of the SIFT features (which may also justify the higher computational time of the comparison step due to the increased size of the features). The second best method, $NTNU_1$, provides a GF2 value of 1.86% which is followed closely by the third and fourth methods ($IDIAP_2$ and $IDIAP_3$) with 2.03%. Nevertheless, it should be highlighted the $NTNU_1$'s significantly smaller processing time for enrolment. Both methods by the $IITIndore$ team provide GF2 values in the order of 6% and when compared to the methods more close to them, $NTNU_3$ and $IDIAP_1$, it can be noted that their processing times for enrolment and comparison are significantly higher. Regarding the **iris task**, observing Table 2, it can be noted that the best method, $NTNU_4$, provided an impressive GF2 value of 0.00%. However, its complexity leads to a high computational time in the template extraction step. After the first ranked, the following methods present much higher error rates: the second method is $NTNU_3$ with 8.43%.

In Figure 2, the DET curves for both tasks are depicted. These curves represent the values of the false non-match rate as a function of the false match rate or in other words, depict the false negatives rate for each value of the false positives rate. Regarding the periocular task, Figure 2(a), it can be observed in these curves that the majority of the methods present a quick decay in the results from GF2 to GF3, exception to be made for the best method, HH_1, which preserves a very low FNMR rate for all values of FMR. Regarding the iris task, Figure 2(b), only two of the methods present a significant increase from GF3 to GF4, the other three out of five methods show comparatively lower values of FNMR for smaller values of FMR.

A comparison between the DET curves of the results obtained in the first and second editions is presented in Figure 3 for each task. Regarding the periocular task, in the *Cross-Eyed2016* competition 2 teams participated with 5 methods and in the *Cross-Eyed2017* this number increased to 12. The comparison is made for the 2 best and 2 worst methods in both editions in Figure 3(a). Regarding the iris task, in the *Cross-Eyed2016* competition only 1 team participated with 3 methods and in *Cross-Eyed2017* 2 teams participated with a total of 5 methods. The best and worst methods from each edition are compared in Figure 3(b). It can be noted that the method's accuracy improved for most the cases, exception to be made for the best periocular method of 2016 which performance, though closely followed, was not overcome by the two best methods of 2017.

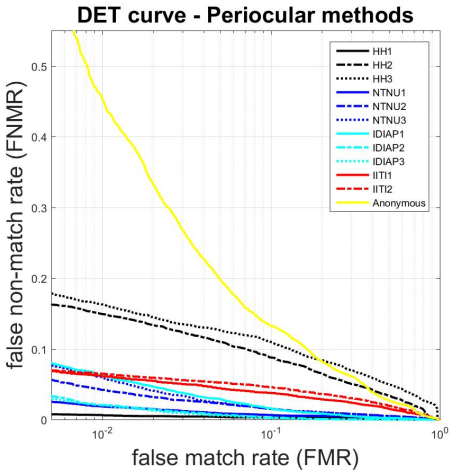

(a) Periocular methods

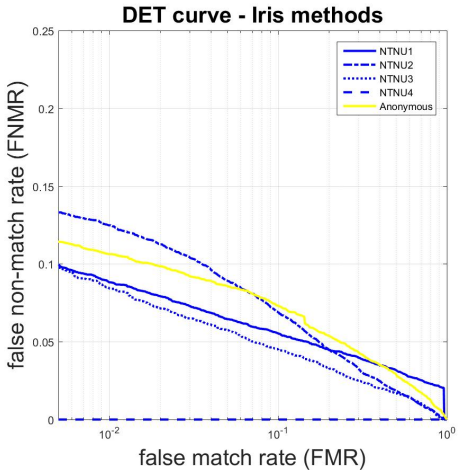

(b) Iris methods

Figure 2. DET curves of the periocular and iris methods.

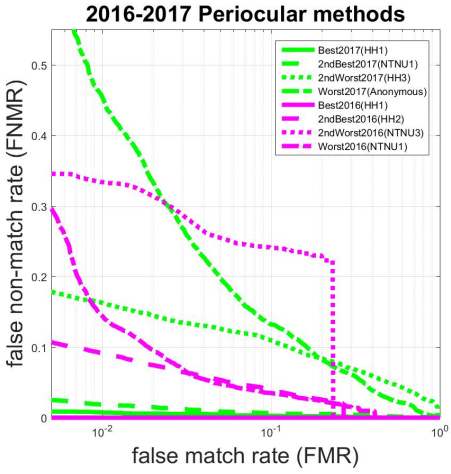

(a) Periocular 2 best and 2 worst methods 2016-2017

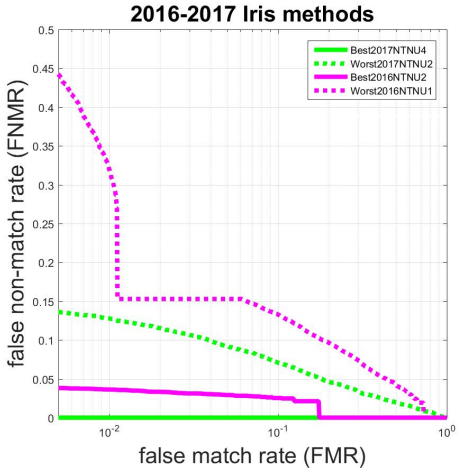

(b) Iris best and worst methods 2016-2017

Figure 3. *Cross-Eyed2016* versus *Cross-Eyed2017*

7. Conclusions

This paper presented the second competition on cross-spectral periocular and iris recognition. This competition and the released training dataset will promote the research on this relatively new topic and provide a valuable dataset of ocular images to the biometric research community. The use of this database will prevail beyond the competition, giving an opportunity for creating spectrum-independent algorithms and evaluating them in experiments. In both periocular and iris tasks, the GF2 values obtained by the best methods are very promising. HH_1 algorithm obtained approximately 99% followed by 4 methods with values of GF2 lower than 5%, for the periocular task. Regarding the iris task, the $NTNU_4$ iris method reached 100.00% GF2 value. Nevertheless, in an overall analysis of all results obtained and the rise of the false non-match rate depicted in the DET curves, it is clear that the cross-spectrum comparison posed a serious challenge to the participants. The results obtained in the two editions of this competition show beyond doubt that this is a not fully investigated problem and much improvement is still expected. The contributions made by the participants in this initiative will open the way to an increased usability of iris/periocular recognition technologies on generic devices and diverse scenarios. It can be noted that many submissions have employed fusion approaches. There are not single-algorithm based submissions tailored for the problem indicating the necessity for continuing research in this topic.

8. Acknowledgements

This work is supported by: FastPass and PROTECT EU projects (grant agreements 312583 and H2020-700259); the Swedish Research Council, and the CAISR and SIDUS-AIR programs of the Swedish Knowledge Foundation; the Research Council of Norway (grant IKTPLUSS 248030/O70); the Swiss National Science Foundation (SNSF) under the HFACE project, the Norwegian SWAN project and the European Community's Seventh Framework Programme (FP7) under grant agreement 284989 (BEAT) and the Swiss Center for Biometrics Research and Testing.

References

[1] M. A. M. Abdullah, J. A. Chambers, W. L. Woo, and S. S. Dlay. Iris biometrie: Is the near-infrared spectrum always the best? In *2015 3rd IAPR Asian Conference on Pattern Recognition (ACPR)*, pages 816–819, Nov 2015.

[2] M. A. M. Abdullah, S. S. Dlay, W. L. Woo, and J. A. Chambers. A novel framework for cross-spectral iris matching. *IPSJ Transactions on Computer Vision and Applications*, 8(1):9, 2016.

[3] F. Alonso-Fernandez and J. Bigun. Near-infrared and visible-light periocular recognition with gabor features using frequency-adaptive automatic eye detection. *IET Biometrics*, 4(2):74–89, 2015.

[4] F. Alonso-Fernandez, J. Fierrez, D. Ramos, and J. Ortega-Garcia. Dealing with sensor interoperability in multi-biometrics: the UPM experience at the biosecure multimodal evaluation 2007. In *Proc. SPIE BTHI*, volume 6944, page 12, 2008.

[5] F. Alonso-Fernandez, P. Tome-Gonzalez, V. Ruiz-Albacete, and J. Ortega-Garcia. Iris recognition based on SIFT features. In *Proc. BIDS*, pages 1–8, 2009.

[6] S. Bharadwaj, H. S. Bhatt, M. Vatsa, and R. Singh. Periocular biometrics: When iris recognition fails. In *Biometrics: Theory Applications and Systems (BTAS), 2010 Fourth IEEE International Conference on*, pages 1–6. IEEE, 2010.

[7] C. Boyce, A. Ross, M. Monaco, L. Hornak, and X. Li. Multispectral iris analysis: A preliminary study. In *Proc. CVPRW*, page 12, 2006.

[8] Z. Cao and N. A. Schmid. Heterogeneous sharpness for cross-spectral face recognition. In *SPIE Defense+ Security*, pages 102020Q–102020Q. International Society for Optics and Photonics, 2017.

[9] Z. Cao, N. A. Schmid, and X. Li. Image disparity in cross-spectral face recognition: mitigating camera and atmospheric effects. In *SPIE Defense+ Security*, pages 98440Z–98440Z. International Society for Optics and Photonics, 2016.

[10] J. M. Dawson, S. C. Leffel, C. Whitelam, and T. Bourlai. *Collection of Multispectral Biometric Data for Cross-spectral Identification Applications*, pages 21–46. Springer International Publishing, Cham, 2016.

[11] B. Gong, Y. Shi, F. Sha, and K. Grauman. Geodesic flow kernel for unsupervised domain adaptation. In *IEEE Conference on Computer Vision and Pattern Recognition (CVPR)*, pages 2066–2073. IEEE, 2012.

[12] M. S. Hosseini, B. N. Araabi, and H. Soltanian-Zadeh. Pigment melanin: Pattern for iris recognition. *IEEE Trans. Instr. Measur.*, 59(4):792–804, April 2010.

[13] International Organization for Standardization. ISO/IEC 19795-1:2006 - Biometric performance testing and reporting – Part 1: Principles and framework, 2006, rev. 2011.

[14] A. K. Jain, N. K. Ratha, and S. Lakshmanan. Object detection using gabor filters. *Pattern recognition*, 30(2):295–309, 1997.

[15] R. Jillela and A. Ross. Matching face against iris images using periocular information. In *Proc. ICIP*, pages 4997–5001, 2014.

[16] J. Kannala and E. Rahtu. BSIF: Binarized statistical image features. In *Proc. ICPR*, pages 1363–1366. IEEE, 2012.

[17] Kiran B. Raja, R. Raghavendra, M. Stokkenes, and C. Busch. Multi-modal authentication system for smartphones using face, iris and periocular. In *Proc. ICB*, pages 143–150, 2015.

[18] Kiran B. Raja, R. Raghavendra, V. K. Vemuri, and C. Busch. Smartphone based visible iris recognition using deep sparse filtering. *Pattern Rec. Lett.*, 57(0):33 – 42, 2015.

[19] A. Mikaelyan, F. Alonso-Fernandez, and J. Bigun. Periocular recognition by detection of local symmetry patterns. In *Proc IEB-SITIS*, pages 584–591, 2014.

[20] P. R. Nalla and A. Kumar. Toward more accurate iris recognition using cross-spectral matching. *IEEE Transactions on Image Processing*, 26(1):208–221, 2017.

[21] H. Ngo, R. Ives, J. Matey, J. Dormo, M. Rhoads, and D. Choi. Design and implementation of a multispectral iris capture system. In *Proc. ACSSC*, pages 380–384, 2009.

[22] V. Ojansivu and J. Heikkilä. Blur insensitive texture classification using local phase quantization. In *International conference on image and signal processing*, pages 236–243. Springer, 2008.

[23] U. Park, R. Jillela, A. Ross, and A. K. Jain. Periocular biometrics in the visible spectrum. *IEEE Trans. Inf. For. Sec.*, 6(1):96–106, 2011.

[24] U. Park, A. Ross, and A. K. Jain. Periocular biometrics in the visible spectrum: A feasibility study. In *3rd IEEE International Conference on Biometrics: Theory, Applications, and Systems (BTAS'09)*, pages 1–6, 2009.

[25] T. d. F. Pereira and S. Marcel. Heterogeneous face recognition using inter-session variability modelling. In *IEEE Computer Society Workshop on Biometrics - CVPRW 2016*, june 2016.

[26] K. B. Raja, R. Raghavendra, and C. Busch. Cross-spectrum periocular authentication for nir and visible images using bank of statistical filters. In *IEEE International Conference on Imaging Systems and Techniques (IST)*, pages 227–231. IEEE, 2016.

[27] N. P. Ramaiah and A. Kumar. Advancing cross-spectral iris recognition research using bi-spectral imaging. In *Mach. Intell. and Signal Proc.*, pages 1–10. Springer, 2016.

[28] N. P. Ramaiah and A. Kumar. On matching cross-spectral periocular images for accurate biometrics identification. In *IEEE 8th International Conference on Biometrics Theory, Applications and Systems (BTAS)*, pages 1–6. IEEE, 2016.

[29] A. Ross, R. Pasula, and L. Hornak. Exploring multispectral iris recognition beyond 900nm. In *Proc. BTAS*, pages 1–8, 2009.

[30] A. F. Sequeira, L. Chen, J. Ferryman, F. Alonso-Fernandez, J. Bigun, Kiran B. Raja, R. Ramachandra, C. Busch, and P. Wild. Cross-Eyed - Cross-Spectral Iris/Periocular Recognition Database and Competition. In *15th International Conference of the Biometrics Special Interest Group (BIOSIG), Darmstadt, Germany.*, volume 6, pages 96–106. IEEE, 2016.

[31] A. F. Sequeira, L. Chen, P. Wild, P. Radu, and J. Ferryman. Cross-Eyed: Reading Cross-Spectrum Iris/Periocular Dataset, 2016. www.crosseyed.eu.

[32] A. Sharma, S. Verma, M. Vatsa, and R. Singh. On cross spectral periocular recognition. In *Proc. ICIP*, pages 5007–5011. IEEE, 2014.

[33] P. Wild, P. Radu, and J. Ferryman. On fusion for multispectral iris recognition. In *Proc. ICB*, pages 31–37, May 2015.

[34] G. Wimmer, T. Tamaki, J. J. Tischendorf, M. Häfner, S. Yoshida, S. Tanaka, and A. Uhl. Directional wavelet based features for colonic polyp classification. *Medical image analysis*, 31:16–36, 2016.